

Thermal energy storage for increased waste heat recovery at a silicon production plant in Norway



Daniel Rohde^a, Anton Beck^b, Paul Wilpert^c, Sabrina Dusek^b, Magnus K. Windfeldt^a, Leif E. Andersson^{a,*}

^a SINTEF Energy Research, Sem Sælands vei 11, 7034 Trondheim, Norway

^b AIT Austrian Institute of Technology GmbH, Giefinggasse 4, 1210 Vienna, Austria

^c Elkem Thamshavn, Byveien 10, 7300 Orkanger, Norway

ARTICLE INFO

Keywords:

Waste heat recovery
Thermal energy storage
Case study
Dynamic simulation
Techno-economic optimization

ABSTRACT

The production of silicon is an energy-intensive process, which requires high temperatures. Sudden release of high-temperature gas to the exhaust system is an inevitable part of silicon furnace operation and causes strong fluctuations in the waste heat recovery system. This makes waste heat recovery challenging and leads to frequent throttling of the produced steam reducing the efficiency of the system. To avoid this throttling and thus increase system efficiency, retrofitting a thermal energy storage to the existing waste heat recovery system is analyzed for a silicon production plant in Norway. A steam accumulator installed in parallel to existing bypasses, which does not interfere with the existing waste heat recovery system, is found to be ideally suited for the case.

The analysis is carried out using real plant data, which is used to calibrate a dynamic simulation model modelled in the Modelica language. Design parameters of the steam accumulator are identified based on economic optimizations and their performance is verified with the dynamic simulation model. The simulation results shows that the simplifications in the economic optimizations are acceptable and that storage sizes of less than 10 m³ can lead to annual profits of around 23 k€. Investment costs excluding transport and on-site installation are around 120 k€, yielding payback times from three to six years, depending on public funds. Including transport and on-site installation increases the payback times to about seven to ten years. The integration of a storage of this size was deemed realistic by the plant operators. The results will therefore be used for the creation of a business case with a more detailed cost analysis.

1. Introduction

Waste heat recovery (WHR) is a key part of improving the efficiency of industrial processes, reducing their fuel consumption and CO₂ emissions. However, in systems where the available heat fluctuates the efficiency of WHR is limited as it might lead to sub-optimal component selection and poor off-design performance [2]. Such process fluctuations are present in many industrial processes including solar thermal power plants [3], steam power units [4], biomass combined heat and power plants [5], steel industry [6], food industry [7] and vehicle applications [8] to name a few. In fact, most industrial processes experience less or more severe fluctuations, which have to be handled by the system.

Thermal energy storages (TES) have been widely investigated for use in industrial WHR [9]. For metal production, focus has been on steel-making plants to improve WHR efficiency both from electric arc

furnaces [6,10,11] and from basic oxygen furnaces [12]. TES can be used to mitigate fluctuation effects and improve the performance of WHR systems and thermal power plants. TES technologies can be categorized into sensible, latent and thermochemical storage system [13]. Sensible storage systems store energy by raising the temperature level of the storage material while latent storage system use phase transition of materials [14]. Thermo-chemical systems store heat through reversible endothermic chemical reactions. A further distinction can be made between active and passive as well as direct and indirect storage systems. In passive storage systems only the heat transfer medium passes through the system for charging and discharging and the storage medium does not circulate, while for active systems the storage medium circulates [13]. In indirect storage system the heat transfer fluid is separated by heat exchangers from the storage medium, while direct systems use the heat transfer fluid directly as storage media [14]. Selecting the most

* Corresponding author.

E-mail address: leif.andersson@sintef.no (L.E. Andersson).

suitable thermal storage solution highly depends on the requirements and characteristics of the process.

A proven technology for TES above 100 °C is the steam accumulator, also known as a Ruths steam storage. Steam is stored directly in a pressure vessel, containing a two-phase fluid of liquid water and steam. A large fraction of the charging steam is condensed and stored as liquid water. During the storage process, the pressure in the vessel increases. Applying a pressure drop when discharging from the storage evaporates the water again and saturated steam is extracted. Since pressure differences are used to store thermal energy in the form of steam, steam accumulators are also referred to as sliding pressure steam accumulators [15].

In solar thermal power plants the coupling between a steam boiler and a steam accumulator is an effective solution to improve the operation of the plant [15–17]. Steinmann and Eck [15] used steam accumulators as a buffer storage system to compensate for fast transients in insulation for solar thermal systems, which are usually not predictable. Moreover, the steam storage helps to limit the thermo-mechanical stress in the components of the power plant due to fluctuations. A numerical simulation model for two-stage thermal energy storage including a steam accumulator and a concrete storage system is presented in Bai and Xu [16].

A technology assessment of different steam storage system for biomass combined heat and power plants (CHP) is given by Stark, Sonnleitner et al. [14]. A detailed investigation of the performance of a steam accumulator together with solid concrete thermal storage and a storage turbine to increase the flexibility of a biomass CHP is presented in Stark, Conti et al. [5]. It is shown that the thermal storage system improves the flexible power production of the plant considerably. Steam accumulators have also been analyzed for improved operation of concentrated solar tower power plants [18], solar desalination plants [19] as well as coal-fired power plants [20]. Biglia, Comba et al. [7] describes the use of steam accumulators in the food industry where steam is supplied discontinuously.

For solar thermal power plants TES are key components to adapt the electricity production to the power demand [3]. The TES solution is usually designed together with the solar thermal power plant and the electricity is the main product of these plants. However, for WHR systems of industrial processes the WHR product is usually considered just a by-product improving the plant's performance. Furthermore, TES is just a measure to improve this by-product. Moreover, WHR and TES solutions must often be retrofitted to existing plants. Consequently, techno-economic challenges such as long payback periods, low profit margins and large investment costs may prevent the implementation of these solutions [2]. Dal Magro et al. [2] designed and simulated a PCM-based storage solution for improving the performance of an organic Rankine cycle for waste heat recovery from a steel billet reheating furnace. The workflow consisted of analyzing real data to find the process characteristics, design and model the system, simulate the original and improved system, and make an economic assessment to estimate the payback period of the thermal storage solution.

Cost-optimized integration of such retrofit solutions in existing systems is crucial to fully exploit WHR potentials. Benalcazar [21] proposed an approach for storage sizing consisting of a heuristic approximation step for storage sizing, an optimization step based on a Mixed-integer linear programming (MILP) formulation to optimize operation and finally a step to evaluate economics of the solution. Pérez-Iribarren, González-Pino [22] investigated optimal design and operation of TES for the use in micro-cogeneration plants to avoid oversizing as early as in the design phase of the CHP. They applied a linear programming-based model to identify optimal component sizes for the system. Both Pizzolato, Donato [23] and Hofmann, Dusek [24] applied nonlinear optimization models (Mixed-integer nonlinear programming (MINLP) and nonlinear programming (NLP)) for optimal sizing of TES without considering operation of the storages directly, but applying factors for assumed cycle durations. Lepiksaar, Mašatin [25] considered

various sensible TES options to increase the flexibility of a CHP plant. They applied simulation-based scenario analysis to identify the best storage solution using the software EnergyPRO. Another MIL(Q)P approach for cost-optimal storage selection and sizing was proposed by Beck, Sevault et al. [26] who considered both TES capacity and heat load requirements in their cost functions.

In this work, the potential of retrofitting a TES system to an existing WHR system at a silicon production plant is investigated. The production of silicon is an energy intensive process and requires high temperatures. About 70% of the energy input leaves the process as thermal energy in cooling water, hot off-gas, by radiation and convection from the furnace, and from the cooling process of liquid silicon [1]. Consequently, WHR systems are key components to improve the efficiency of the process and reduce fuel consumption and CO₂ emissions of silicon plants [27]. Important properties of the retrofit solution are that it is simple to integrate into the existing WHR system, does not influence the silicon production nor jeopardize the performance of the WHR system while improving its flexibility. According to the plant operators, low payback periods are critical for new investments due to low margins and uncertainties in future operation. A combined approach of techno-economic optimization and dynamic system simulation was chosen for this case study. Real plant data is used to calibrate a simulation model, optimize the TES in a techno-economic optimization and compare the performance of the WHR system with and without TES in a simulation model.

The remainder of this paper is structured as follows: a description of the challenges for the WHR system in silicon and ferrosilicon production processes and an introduction of the considered case study system is given in Section 2. In Section 3, the methodology for simulation and optimization is explained, followed by a presentation of results in Section 4. The paper ends with a conclusion in Section 5.

2. Problem description

In silicon production processes silicon is produced by reduction of silicon dioxide with carbon in a submerged arc furnace (Fig. 1). Temperatures above 1800 °C are required to achieve the reduction. The heating of the process is achieved by electric energy. The off-gas from the furnace consisting of SiO and CO is mixed with excess air under the furnace hood and burned [27]. Moreover, these high-temperature gases, which are formed in the lower part of the furnace, interact with charge material while rising. However, the gas is often trapped in cavities surrounding the electrodes because the charge material tends to agglomerate when heated [28]. As pressure builds up in these cavities, channels may form through which the gas escapes to the surface. Consequently, the gas escapes the furnace at high temperatures and without reacting with the charge, which reduces both the silicon yield and the energy efficiency of the furnace. In addition, the pressure build-up is a safety concern so the cavities are regularly collapsed by manual stoking of the furnace [29]. Thus, the sudden release of high-temperature gas to the exhaust system, either from the stoking process or the gas channel formation, is an inevitable part of silicon and ferrosilicon furnace operation. These temperature fluctuations make WHR from the furnace off-gas challenging. Moreover, if a WHR system is implemented, the system must manage large variations in the boiler duty (Fig. 2). TES can mitigate temperature and boiler duty fluctuations and thus ease the process operation, reduce thermal stress on components and increase the efficiency of the WHR system in a silicon plant.

2.1. The case study

Elkem Thamshavn is a global vendor for advanced silicon products and Microsilica™, located in Mid-Norway (Fig. 3). The plant is one of the world's most energy efficient silicon plants due to its advanced energy recovery system, which recovers heat from the off-gas of the two silicon furnaces for electricity generation and heat export. The WHR

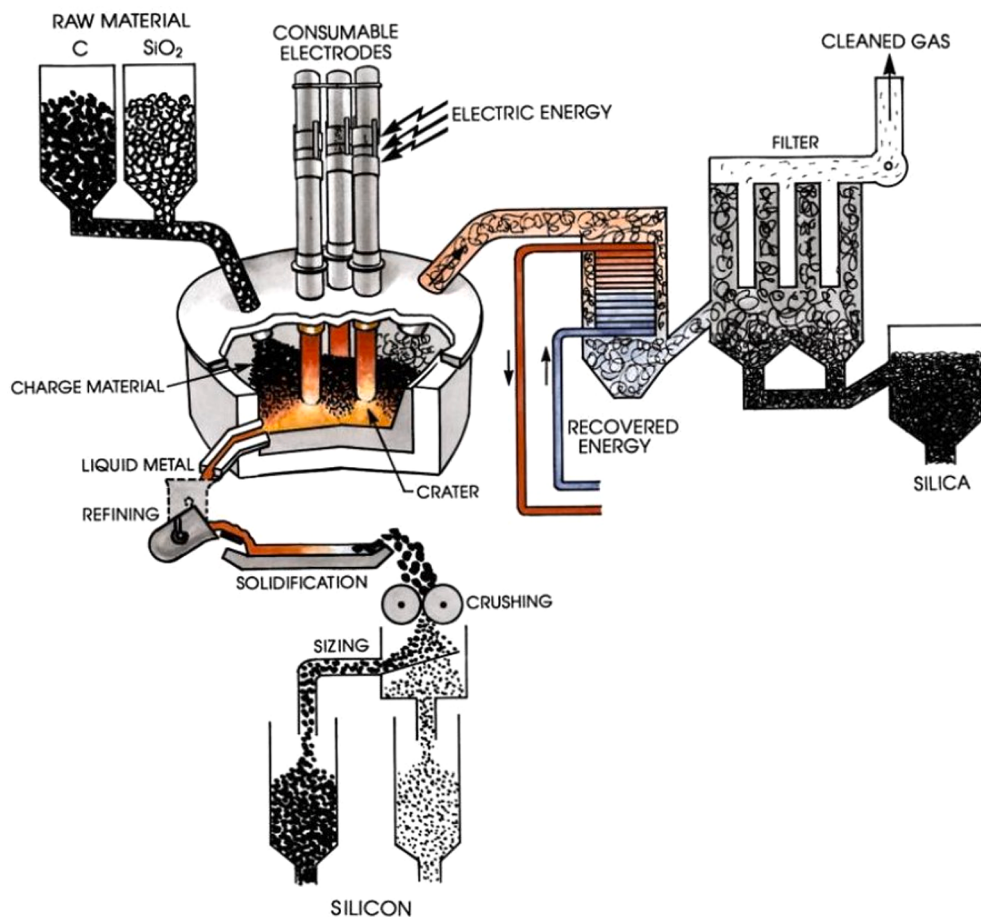


Fig. 1. Schematic drawing of a typical silicon production process [1].

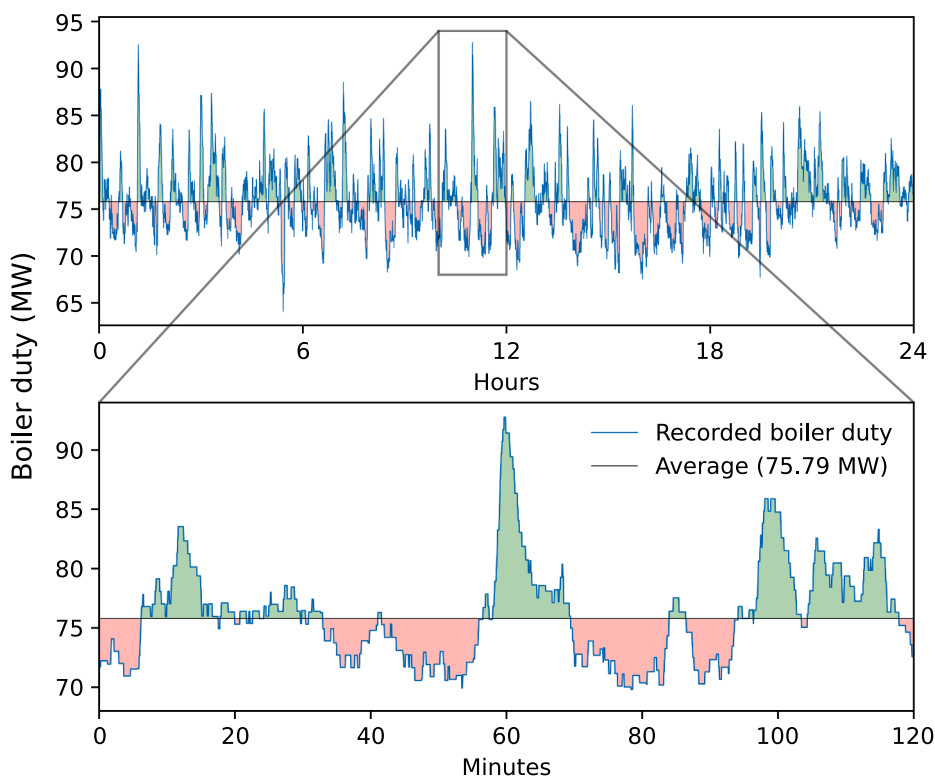


Fig. 2. Example of variations around the average boiler duty in the Elkem Thamshavn silicon plant.



Fig. 3. Elkem Thamshavn.

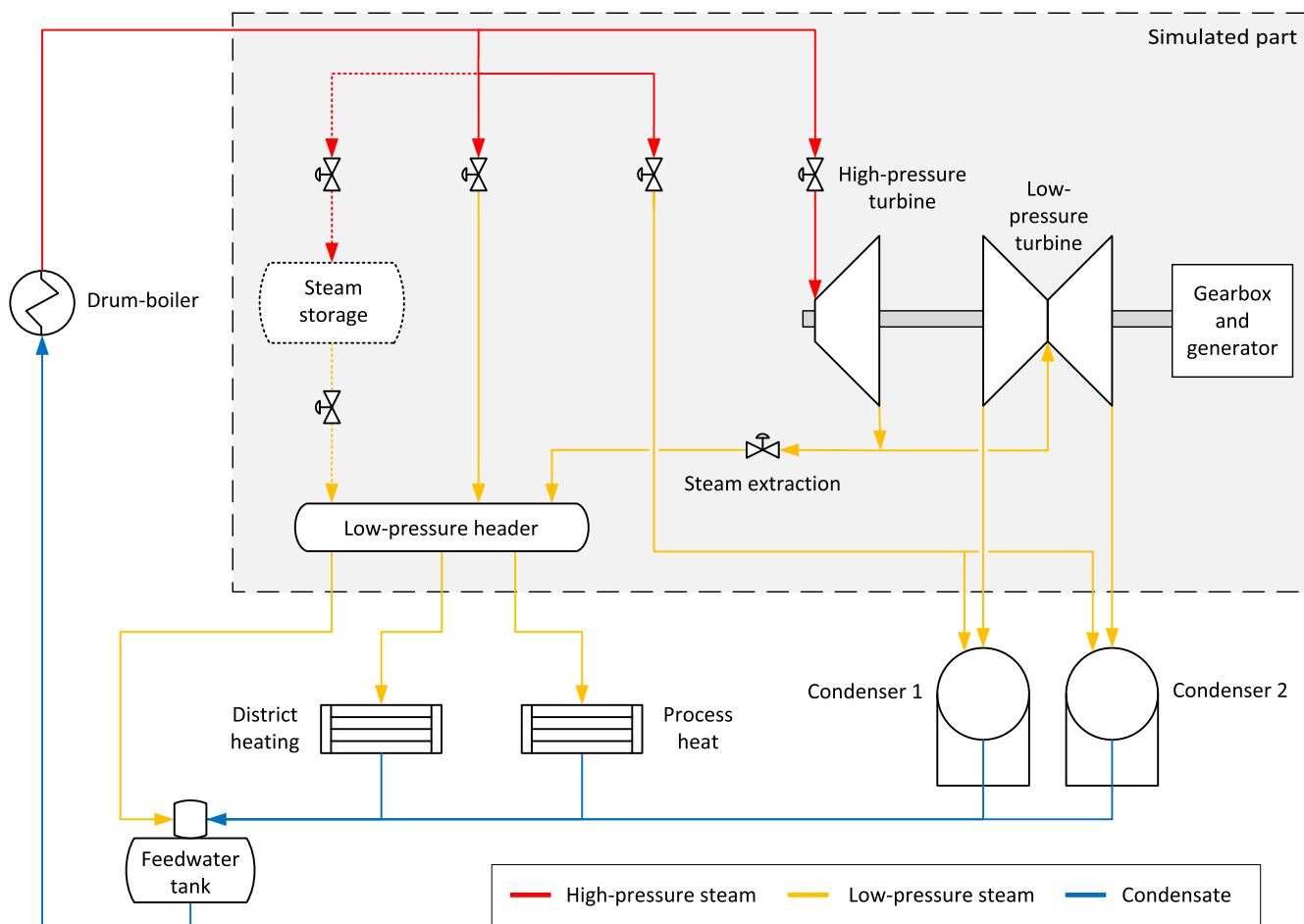


Fig. 4. Schematic of the energy recovery system at Elkem Thamshavn (drum-boiler system oversimplified, water injection and water refill of the storage omitted for clarity). The dashed lines show the potential storage implementation.

system is described in detail in Section 2.1.1.

2.1.1. The existing waste heat recovery system

The WHR system dates as far back as 1986 and has played a key role in the economic operation of the plant and has undergone continuous improvements. In 2000, a steam hood for Furnace 1 was installed [30], which functions as an additional evaporator. In 2012, the system was significantly upgraded by installing several new heat exchanger sections, replacing the low-pressure turbine rotor, and installing a new generator. A schematic of the WHR system downstream of the drum boiler is shown in Fig. 4.

The off-gas from the two silicon furnaces is directed through a common drum-based boiler system, which consists of two drums and several heat exchanger sections (economizers, evaporators, and superheaters). The produced steam from this drum-boiler and the steam hood of Furnace 1 is used to power a 22 MW extraction turbine, which drives an electric generator, and as heat supply for a low-pressure header. The steam supply of the low-pressure header is prioritized over the steam turbine in case of low steam pressure from the boiler. The steam for the low-pressure header is further utilized to supply heat to a district heating network, for feedwater preheating and as process heat (Fig. 4).

In normal operation superheated steam is first sent to the high-pressure turbine. Afterwards stream is extracted from the outlet of the high-pressure turbine to supply the low-pressure header. The remaining steam is sent to the low-pressure turbine. The steam at the outlet of the low-pressure turbine is sent to sea-water cooled condensers, which condense the steam at a temperature of 36 °C and a pressure of around 6 kPa. Currently, the system produces around 150 GWh of electrical energy and supplies around 15 GWh of heat to the local district heating network per year [31].

The temperature range of the off-gas entering the boiler is usually between 700 and 800 °C. However, temperature spikes of up to 1400 °C occur regularly when gas bubbles in the furnaces collapse. These temperature spikes lead to an overproduction of steam, i.e., more steam is generated than can be expanded in the high-pressure turbine. If possible, the excess steam is sent to the low-pressure header, which allows to reduce the extraction behind the high-pressure turbine. Otherwise, excess steam is bypassed directly to the condensers. This direct steam throttling to the condensers results in an undesirable loss of recovered energy, which is about 1.5 GWh per year.

2.1.2. The retrofitted TES solution

TES solutions were proposed for the steel industry that also suffers from temperature variations of the flue gas. However, the time scales in the silicon production process are usually shorter. Moreover, a major difference to similar studies, e.g. Dal Magro, Jimenez-Arreola [2], Nardin, Meneghetti [6], is the location of the TES solution. In this study a TES should be retrofitted to an existing WHR system to reduce or even avoid the throttling of the turbine. Therefore, the TES solution in this paper mitigates fluctuations in the steam mass flow coming from the drum-boiler and not temperature variations in the flue gas. Therefore, a Ruths steam storage was chosen, which is a direct thermal storage system.

The proposed integration of the steam storage into the system is shown with dashed lines in Fig. 4. Discharging steam from the storage to the low-pressure header reduces the need for steam extraction behind the high-pressure turbine and thus increase electricity production. The steam storage can be installed in parallel to the other bypasses and does not interfere with plant regulations, which favor adding new components without changing existing parts of the system. The chosen position also experiences a large pressure difference between charging and discharging, which is beneficial for storage tank compactness. Furthermore, pressure directives require steam storage inspections, which are easiest with the proposed configuration.

2.2. Data acquisition

The WHR control system is equipped with a data acquisition system that saves data for the previous six months. The control system has about 10.000 sensor nodes connected to a few programmable logic controllers (PLC) for the furnaces and WHR system. Temperatures and pressures are measured directly, values for mass flow rates are calculated by the control system based on pressure drop measurements. A representative week of operation was selected by the plant operators and measurement data for this week were retrieved and processed for the analysis.

Figs. 5–8 show measured data for the steam temperature, the steam pressure, the steam mass flow rates, and the produced electricity of the WHR system for the selected week, respectively.

3. Methodology

The following methodology to design and evaluate the performance of the TES was adopted, as illustrated in Fig. 9.

First, data was received from the silicon plant and the performance of the WHR was analyzed to estimate the potential improvements of the WHR by installing a TES. Moreover, the data was downsampled to make it manageable in simulation and optimization. Second, a dynamic simulation model of the existing WHR was created. The model was calibrated using real data, which guaranteed that the steam flow to the low-pressure header, the steam flow to the condenser and the steam flow extracted from the high-pressure turbine align with measured data. The latter was not measurable directly in the plant and was estimated by aligning measured and simulated power production in the steam turbine generator.

Third, the measured data and estimated streams from the calibrated simulation model were used in a techno-economic optimization to find optimal designs of a Ruths steam storage. It is important to design a storage according to the process at hand because the storage capacity defines how the storage can be operated. From a technical perspective, the efficiency of the plant would be maximized if steam throttling would be avoided completely. However, this would require a relatively large storage, which might not be the best option from an economic perspective. Therefore, techno-economic optimizations of different scenarios were performed in this study. The output of the techno-economic optimization were design parameters of the Ruths steam storage that were used to parameterize a simulation model of the WHR including a steam accumulator. Finally, the simulation models were used to compare and analyze the performance of the original and retrofitted WHR system. In the following sections the dynamic system simulation, the techno-economic storage optimization and the different scenarios used in the optimization, and the control logic for the retrofitted WHR system are described in more detail.

3.1. Dynamic system simulations

The dynamic simulation model is required to estimate non-measurable streams and produces inputs to the techno-economic optimization. In addition, it is used to compare the performance of the base case without TES with the scenarios with TES. The techno-economic optimization also calculates the storage performance, but during the optimization the data for the entire analyzed period is known to the solver. Charging and discharging behavior is, therefore, based on perfect prediction. This makes the optimization result an upper bound of what can be achieved in practice. In addition, steam coming from the drum-boiler system is assumed in the optimization to enter the storage with constant enthalpy. Therefore, the dynamic system simulations are performed to validate and compare feasible and cost-efficient operation of the optimized storage designs.

3.1.1. The heat recovery system model

The heat recovery system was modeled using the object-oriented,

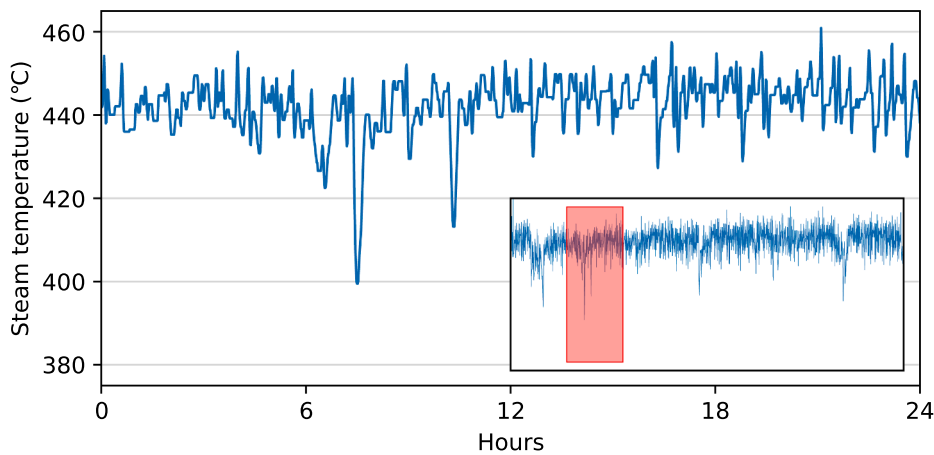


Fig. 5. Measured steam temperature from the drum-boiler.

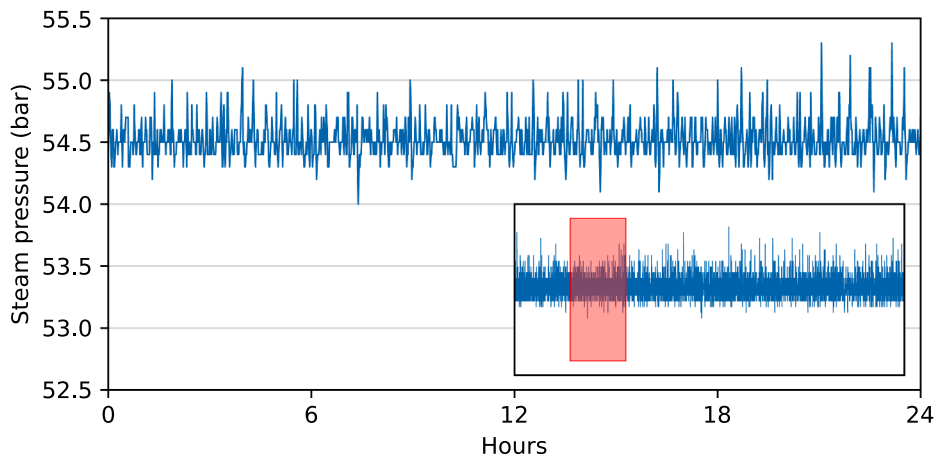


Fig. 6. Measured steam pressure from the drum-boiler.

open-source modeling language Modelica. Dymola Version 2021 was used as simulation environment. The simulated domain was limited to the part relevant for storage operation (Fig. 4). The simulation model with TES is shown in Fig. 10. The low-pressure header and the condensers were not modeled since their operation is uncritical and does not affect the operation of the storage. Instead, constant pressures of 3.5 bar and 0.06 bar were assumed for the low-pressure header and the condensers, respectively. The components used in the system model are described below.

In the system model, basic components from the commercial library TIL from TLK Thermo GmbH [32] were used and specified in close dialogue with the plant operators. The turbine model described in Rohde, Andresen [31] was used in this study. It is based on Stodola's law of cones and a constant isentropic efficiency of 0.87. The high- and low-pressure part of the turbine were modeled separately to allow for steam extraction.

The Ruths steam storage model (labeled "TES" in Fig. 10) was the key component in the system model. This model was developed when investigating a hybrid storage concept, which combines a Ruths steam storage with phase change material [33,34]. However, in this work the Ruths steam storage model without phase change material is used. In Dusek and Hofmann [33], Dusek and Hofmann [34] a validation of the Ruths steam storage model is presented.

As shown in Fig. 11, the model consists of a two-phase fluid volume surrounded by a pressure vessel wall, an insulation layer, and an outer plate. All parts were modeled as cylindrical elements in horizontal orientation with flat adiabatic side-faces. Heat losses were therefore

only taken into account via the cylindric shell surface of the storage. In the two-phase fluid volume, thermodynamic equilibrium between the liquid and the steam phase was assumed. Heat transfer to the pressure vessel wall was modeled with a constant heat transfer coefficient of 1000 W/(m²•K). In the wall, the insulation layer, and the outer plate, heat conduction and the sensible storage capacity of the materials were modeled (Table 1). Heat transfer from the outer plate to the ambient was included in the model with a constant heat transfer coefficient of 5 W/(m²•K) and a constant ambient temperature of 15 °C.

3.2. Techno-economic storage optimization

In order to identify optimal storage sizing in terms of storage capacity, operating temperature range and maximum heat load requirements, a quadratic programming model was used to minimize costs of the WHR system consisting of the TES unit and the steam turbine.

3.2.1. Objective function

The objective function is set to minimize the total annual costs, which are a trade-off between investment costs of the storage and the additional revenues from operation with increased plant efficiency.

$$obj = \min \left(\frac{C_{\text{invest}}^S}{y} (1 - \text{discount}) - \sum_{t \in \text{NOP}} \dot{Q}_t^{\text{out}} \frac{\text{gains}_{LP}}{h^E} \Delta t \frac{\text{duration}}{365} \text{prof}_{\text{spec}} \right) \quad (1)$$

Here, y is the annualization period, discount is the discount rate and duration is the analyzed period. The index t represents the operating

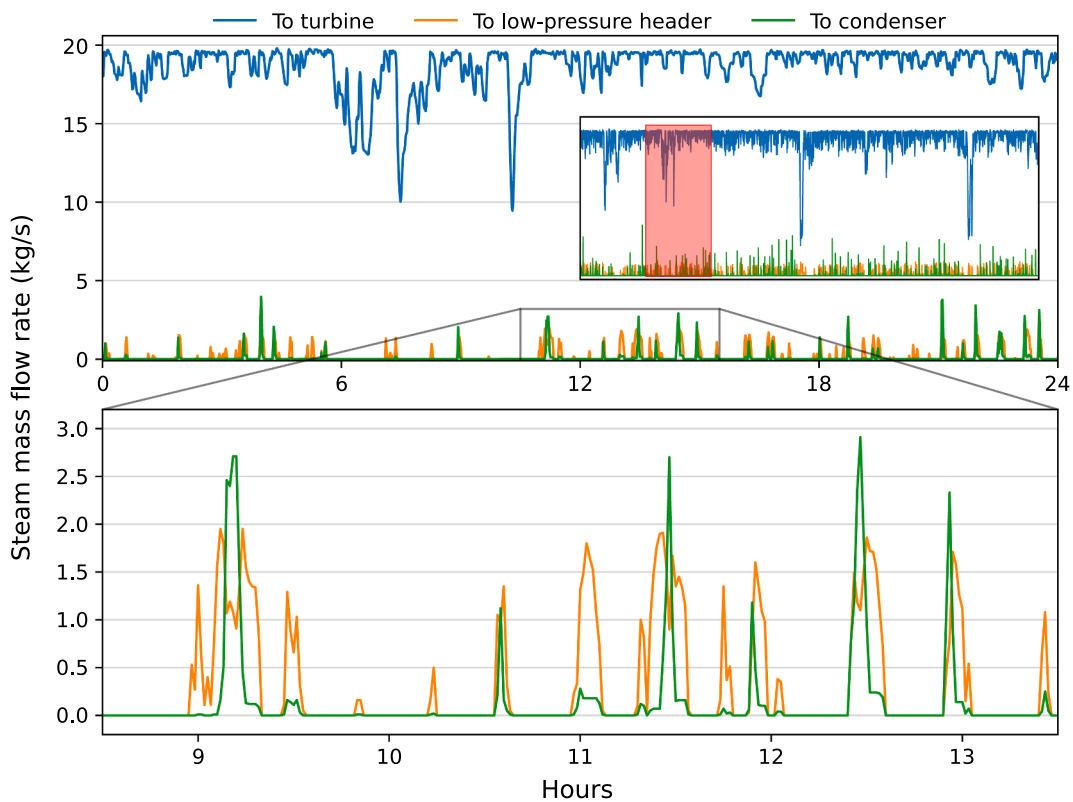


Fig. 7. Measured distribution of steam mass flow rate from drum-boiler.

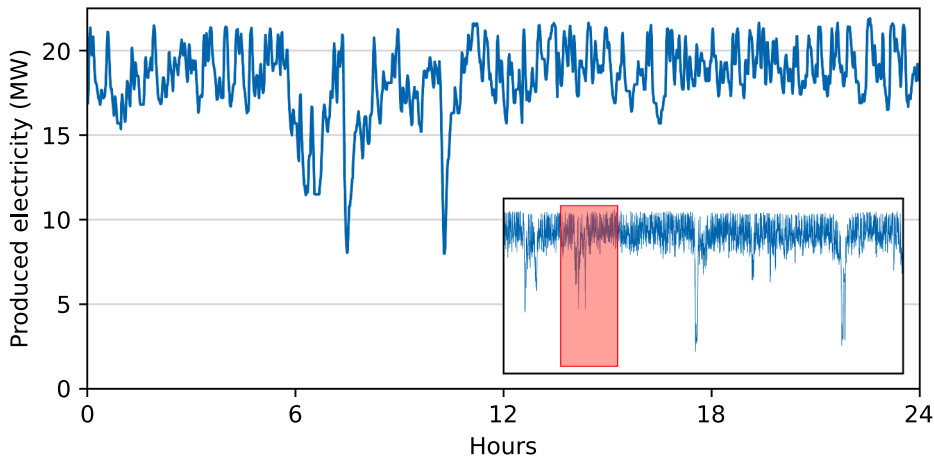


Fig. 8. Measured electricity production of the generator.

periods and NOP is the set of all these time periods. The remaining elements of the objective function are described in the following sections.

3.2.2. Storage investment costs

Many approaches for cost optimization of TES rely on predefined cost parameters, although the actual TES requirements can have a significant impact on TES investment costs [26]. Performance and costs of the individual storage highly depend on various requirements, e.g., temperature range, case specific restrictions, heat loads, and capacities. Algorithms for the generation of such tailored cost functions were proposed in [26] and were used in this study as explained below.

Costs for the Rouths steam storage were calculated by varying storage size, maximum heat load and maximum storage temperature and calculating the resulting storage costs based on information from the pressure vessel database CE 2000 and additional vendor specific costs

for valves and instrumentation. The costs considered for Rouths steam storages were vessel costs, insulation costs, valve and instrumentation costs, and a profit surcharge of 30%. Vessel costs depend on storage size and required wall thickness, which is driven by maximum storage pressures. Insulation costs depend on the storage surface area and the maximum temperature within the storage. Valve costs depend on volume flow rate and pressure. The pressure for the charging valve is defined by the steam pressure from the drum boiler and pressure for the discharging valve by the maximum storage pressure. For this study, the maximum storage temperature was set to 268.8 °C, corresponding to the saturation temperature of the steam supplied by the drum-boiler (54 bar, 450 °C). The minimum storage temperature was set to 138.9 °C, corresponding to the pressure of the low-pressure header (3.5 bar) to which the discharged steam would be sent. The data points obtained from parameter variations for all configurations are shown in Fig. 12.

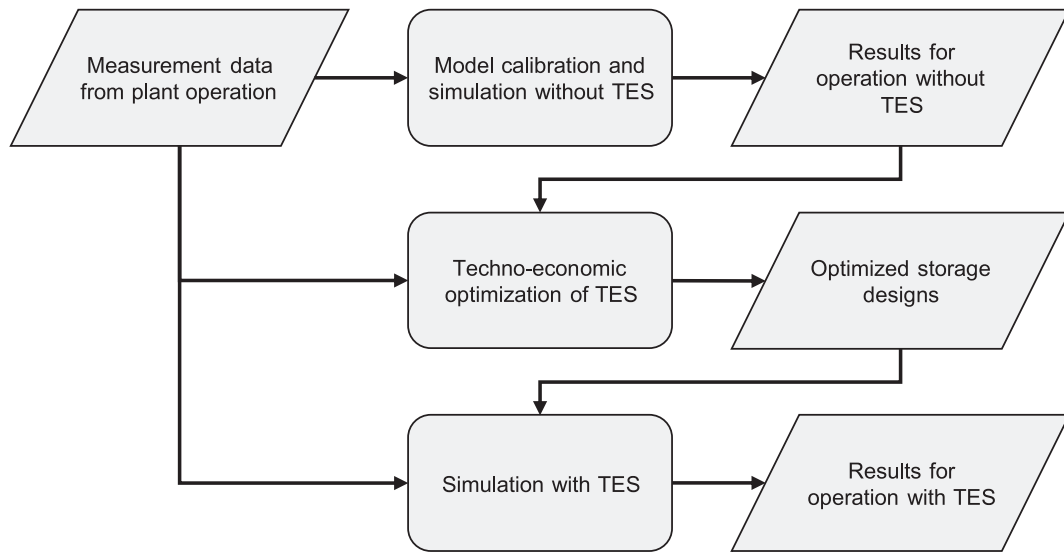


Fig. 9. Methodology of designing and evaluating the TES.

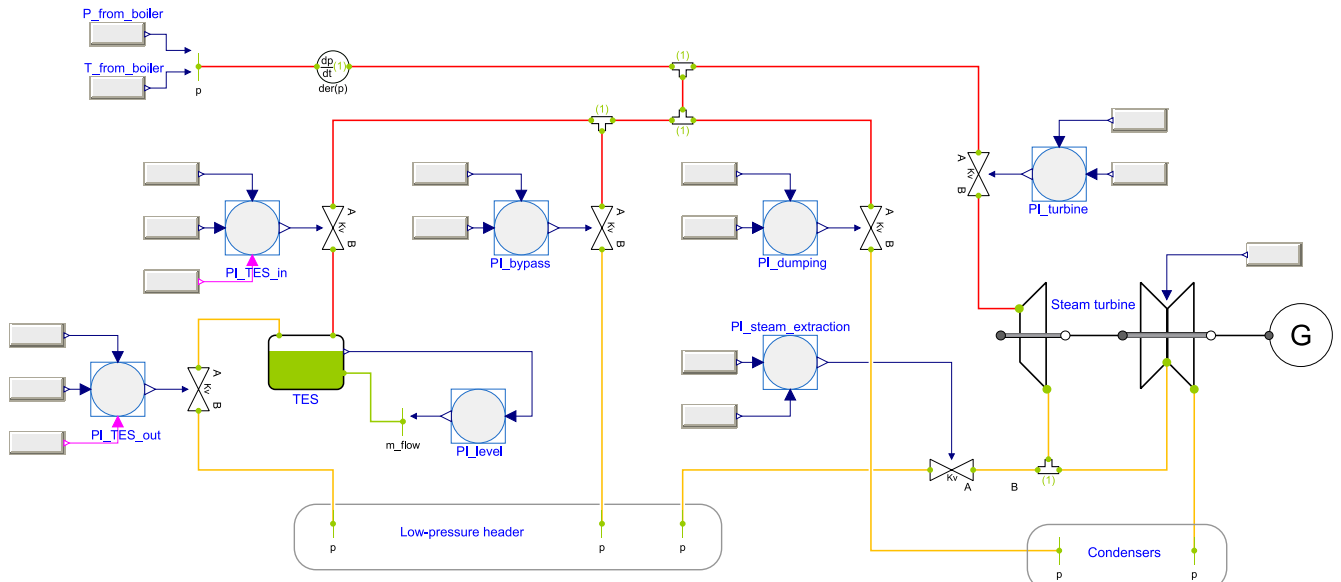


Fig. 10. Schematic of the system model with TES in Dymola.

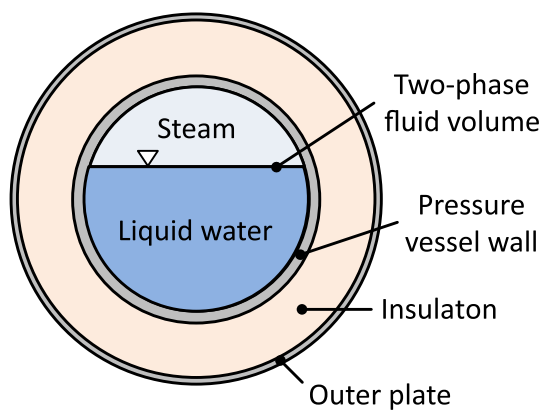


Fig. 11. Main elements of the Ruths steam storage model.

Table 1
Parameters of the Ruths steam storage.

	Pressure vessel wall	Insulation	Outer plate
Thickness	mm	50	400
Density	kg/m ³	7800	80
Specific heat capacity	J/(kg•K)	490	840
Thermal conductivity	W/(m•K)	50	0.035
			50

The coefficients for a quadratic cost function were then defined by means of a least square fit through all data points (Fig. 12). This function defines the investment costs (total costs) C_{invest}^S based on storage capacity (ΔQ^S) and maximum heat load ($\dot{Q}^{S,\text{max}}$) as shown in Eq. (2):

$$C_{\text{invest}}^S = c_0^S + c_1^S \Delta Q^S + c_2^S \dot{Q}^{S,\text{max}} + c_3^S \Delta Q^S \dot{Q}^{S,\text{max}} + c_4^S \Delta Q^{S^2} + c_5^S \dot{Q}^{S,\text{max}^2} \quad (2)$$

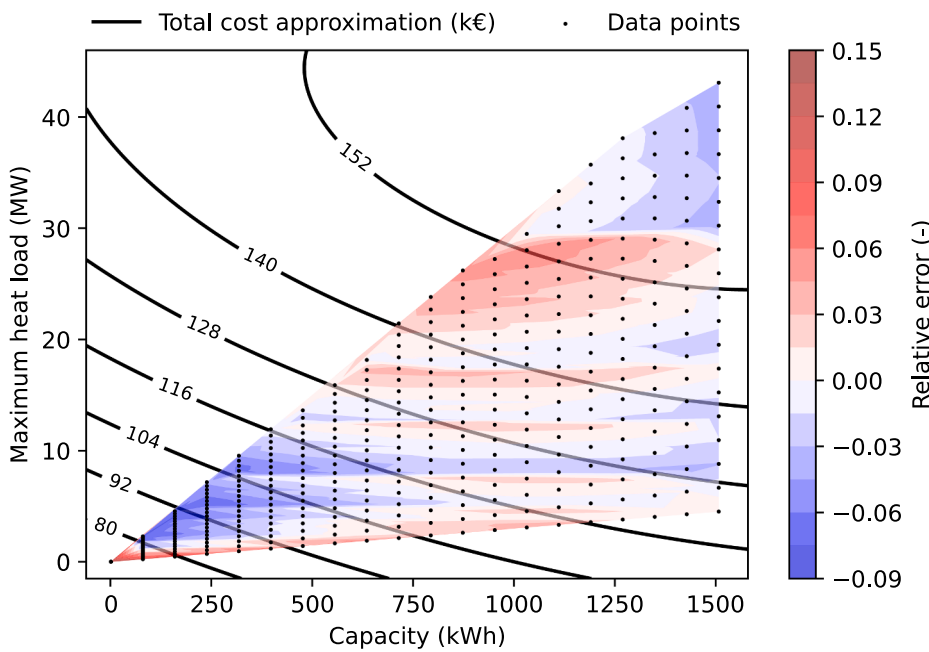


Fig. 12. Data points (black dots) for cost function calculation and quadratic approximation (Eq. (2)). $R^2: 0.979$, $c_0: 72009$, $c_1: 44.44$, $c_2: 2.95$, $c_3: -0.011$, $c_4: 0$, $c_5: -0.00038$.

This cost function was used in the objective function (Eq. (1)) of the optimization problem. The cost function shows decreasing specific costs with storage size and thus forms a nonconvex function. After the optimal design is found, the cost function algorithm is used to recover the actual storage design specifications such as vessel volume, wall thickness, valves, etc. by identifying the data point closest to the optimal solution satisfying capacity and maximum heat load. The optimization problems were solved using CPLEX 12.9.0.0.

3.2.3. Additional revenues from plant operation with storage

Plant operation with storage would allow to discharge stored steam to the low-pressure header, leading to reduced steam extraction from the turbine and thus increased electricity production (Fig. 4). The additional revenues were therefore calculated based on the amount of discharged steam (\dot{Q}_t^{out}), the increased electricity production due to discharging ($gains_{LP}$) and the profits from increased electricity production ($prof_{spec}$) as explained below.

The operation of the storage was calculated based on energy balances, with the optimum capacity and the maximum heat load being a result of the optimization. The available storage capacity ΔQ^S was defined as:

$$\Delta Q^S = Q^{S,max} - Q^{S,min} \quad (3)$$

Bounds for capacity ΔQ^S and heat loads $\dot{Q}^{S,max}$ constrain the domain in the optimization problem to the approximation domain of the cost-function:

$$\Delta Q^S \leq \Delta \dot{Q}^{S,max} \quad (4)$$

Maximum heat load with respect to the actual storage capacity ΔQ^S with the heat load ratio r (maximum charging and discharging ratio in 1/h):

$$\Delta Q^S r \geq \dot{Q}^{S,max} \quad (5)$$

Maximum heat loads for charging ($\dot{Q}^{S,max,c}$) and discharging ($\dot{Q}^{S,max,d}$) were set to:

$$\dot{Q}^{S,max,c} \geq \dot{Q}_t^{S,in} - \dot{Q}_t^{S,out}, \forall t \in NOP \quad (6)$$

$$\dot{Q}^{S,max,d} \geq \dot{Q}_t^{S,out} - \dot{Q}_t^{S,in}, \forall t \in NOP \quad (7)$$

The current state of charge Q_t^S was based on the previous time step and the incoming and outgoing heat loads:

$$Q_{t=1}^S = Q_{t=NOP}^S + \left(\dot{Q}_{t=NOP}^{S,in} - \dot{Q}_{t=NOP}^{S,out} \right) \Delta t \quad (8)$$

$$Q_{t+1}^S = Q_t^S + \left(\dot{Q}_t^{S,in} - \dot{Q}_t^{S,out} \right) \Delta t - \frac{Q_t^S + Q_{t+1}^S}{2} \Delta t q_{loss}, \quad \forall t \in NOP \quad (9)$$

with $q_{loss} = 0.001$ kW/kWh and $Q_{t=1}^S = 0$. The current energy content within the storage Q_t^S had the upper and lower limit $Q^{S,max}$ and $Q^{S,min}$, respectively:

$$Q^{S,max} \geq Q_t^S \geq Q^{S,min}, \forall t \in NOP \quad (10)$$

The charging energy flow rate was constrained by the available excess steam \dot{m}_t^{excess} :

$$0 \leq \dot{Q}_t^{in} \leq \dot{m}_t^{excess} h_{boiler}, \forall t \in NOP \quad (11)$$

The discharging mass flow rate was constrained by the steam demand, i.e. the mass flow rate of stream extraction $\dot{m}_t^{extraction}$ and its corresponding specific enthalpy h^E . In addition, it was assumed that discharging is only possible if no excess steam is available.

$$0 \leq \dot{Q}_t^{out} \leq \dot{m}_t^{extraction} \left(1 - sign(\dot{m}_t^{excess}) \right) h^E, \quad \forall t \in NOP \quad (12)$$

The specific steam enthalpies for charging and discharging were set to the following values for all optimizations:

- Steam from drum-boiler: $h_{boiler} = 3311.5$ kJ/kg
- Steam to low-pressure header (3.5 bar, saturated steam): $h^{LT} = 2732.0$ kJ/kg
- Steam from turbine extraction (7.5 bar, superheated steam): $h^E = 2924.4$ kJ/kg

Based on the measurement data, the specific gain of the low-pressure turbine, i.e., the additional electricity that is produced for each additional kilogram of steam, was set to $gains_{LP} = 0.1284 \text{ kWh}_{el}/\text{kg}$. The specific profits, i.e., the profits per produced MWh of electricity, were set to $prof_{spec} = 47.47 \text{ €}/\text{MWh}_{el}$ based on information from the plant operators.

3.3. Scenarios for the techno-economic optimization

Besides economic parameters for storage sizing, two economic parameters for the WHR system were inputs to the optimizations:

- discount rate
- annualization period.

Industry can apply for public funds in Norway when implementing energy efficiency measures. This funding directly reduces the investment costs and thus the payback period. Three different discount rates, namely 0%, 20%, and 50%, were chosen for this study. The annualization period defined the number of years over which the investment costs were divided. Three different annualization periods, namely 5, 10, and 15 years, were chosen for this study.

3.4. System simulations with optimized storage designs

The techno-economic optimization defines for the simulation the storage size, the maximum pressure level and charging and discharging mass flow rate for each scenario. The storage was assumed to be cylindric and the volume from the optimization was translated to a length and a diameter. The discrete values of volume, length, and diameter for pressure vessel given in [35] were used and interpolated to receive reasonable ratios between length and diameter of the vessel. The control strategy was based on the available excess steam, the demand for steam extraction, and the current pressure in the storage as shown in Fig. 13. This strategy was implemented in the system model using blocks from the library StateGraph, which is included in the Modelica Standard Library.

The size of the valve from drum-boiler to steam storage defined the maximum mass flow rate during charging of the storage. The size was a result from the optimization and was set accordingly for the different scenarios. The mass flow rate during discharging was controlled to satisfy the steam demand at the low-pressure header but was also limited by the discharging valve size found during optimization. As explained earlier, discharging of the storage reduced the need for steam extraction

behind the high-pressure steam turbine and thus led to increased electricity production in the low-pressure turbine. To calculate this increase in electricity production, the results from the storage case simulations were compared to a base case simulation, in which the storage was not used. Thus, the difference between the cases was solely due to the effect of the different storage designs and therefore ensured a fair comparison. The result of the techno-economic optimization and comparisons of the base case without TES and the case with TES are presented in the next section.

4. Results and discussion

First, the results of the techno-economic optimization are presented. The techno-economic optimization defines the design parameters of the TES, which are used in the simulation. Furthermore, the optimization gives an upper bound on the performance of the TES. Second, the simulation results are presented and compared with the results of the optimization.

4.1. Result of the techno-economic optimization

Results from the optimization procedure described in Section 3.2 for all nine scenarios (Section 3.3) are listed in Table 2.

It can be seen from Table 2 that the storage volume (inner vessel volume) ranged from 2.9 to 9.2 m³ with capacities ranging from 414 to 1189 kWh. The maximum storage temperature and maximum storage pressure, which are directly coupled due to the two-phase region the steam accumulator operates in, vary between 256 °C and 269 °C and 4.4 and 5.4 MPa, respectively. The charging flow rate varies between 2.1 and 4.2 kg/s and the discharging flow rate between 2.5 and 3.0 kg/s. The implementation of a TES could recover 84 to almost 99% of the available excess steam. However, a storage volume of 4.2 m³ already allows to recover about 93% of the excess steam. Increasing the amount of recovered steam requires a considerable larger storage volume. To recover about 98% of the excess steam a storage volume of more than 9 m³ is required. Interestingly, the dimension of the inlet and outlet valves vary less significantly. In fact, the maximum flow rate of the outlet valve is the same for all scenarios besides scenario 1. Indeed, in all scenarios but scenario 1 the optimization chooses the largest possible outlet valve since the discharge flow rate was constrained to be smaller than 3.0 kg/s. The vessel and valve dimensions in scenario 1 are smaller than in the other scenarios, which reduces the costs but also the profits.

The non-discounted costs vary between 108 and 137 k€ for all scenarios. A breakdown of the costs is shown in Fig. 14.

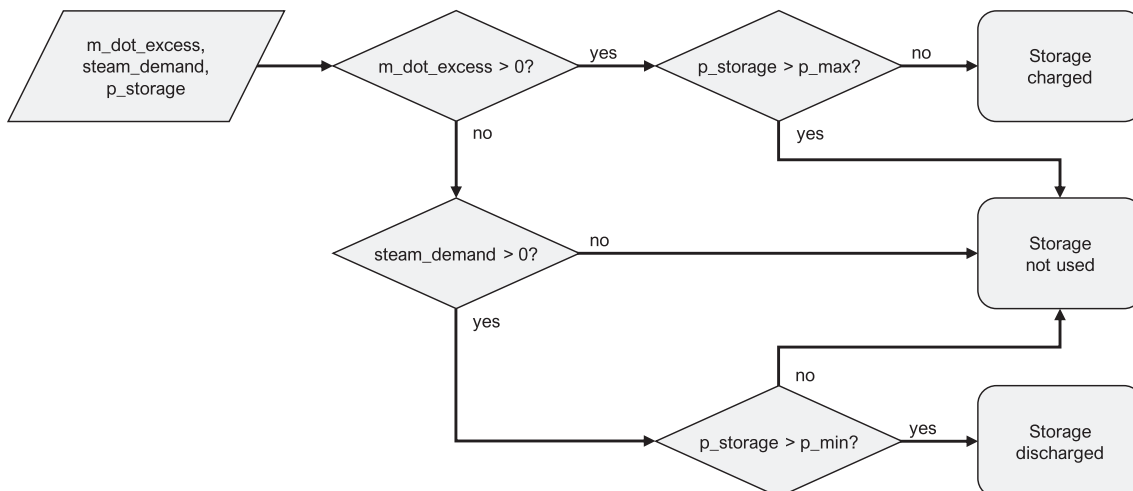


Fig. 13. Storage control strategy implemented in the dynamic system model, where m_{dot_excess} is available excess steam, $steam_{demand}$ is the demand for steam extraction, $p_{storage}$ is the current pressure in the storage and p_{max} and p_{min} are the maximum and minimum storage pressures.

Table 2
Storage optimization result overview.

Scenario Nr.		1	2	3	4	5	6	7	8	9
Discount factor	%	0	0	0	20	20	20	50	50	50
Annualization period	y	5	10	15	5	10	15	5	10	15
<i>Design Parameter</i>										
Storage volume	m ³	2.9	4.2	6.9	4.2	5.1	9.1	4.2	9.1	9.2
Length	m	1.6	1.7	2.0	1.7	1.8	2.1	1.7	2.1	2.1
Diameter	m	1.5	1.8	2.1	1.8	1.9	2.3	1.8	2.3	2.3
Storage capacity	kWh	414	601	889	601	726	1179	601	1179	1189
Max. storage temperature	°C	268.8	268.8	255.8	268.8	268.8	255.8	268.8	255.8	255.8
Max. storage pressure	MPa	5.4	5.4	4.4	5.4	5.4	4.4	5.4	4.4	4.4
Max. charge flow rate	kg/s	2.1	3.1	3.8	3.1	3.2	4.0	3.1	4.0	4.2
Max. discharge flow rate	kg/s	2.5	3.0	3.0	3.0	3.0	3.0	3.0	3.0	3.0
<i>Economic Results</i>										
Non-discounted storage costs	k€	108.1	120.9	131.3	120.9	123.3	136.5	120.9	136.5	136.7
Discounted storage costs	k€	108.1	120.9	131.3	96.7	98.6	109.2	60.4	68.3	68.4
Recovered excess steam	%	84.3	92.9	96.7	92.9	94.4	98.3	92.9	98.3	98.5
Annual profits	k€/y	20.5	22.6	23.6	22.6	23.0	24.0	22.6	24.0	24.0
Discounted payback time	y	5.3	5.3	5.6	4.3	4.3	4.6	2.7	2.9	2.8

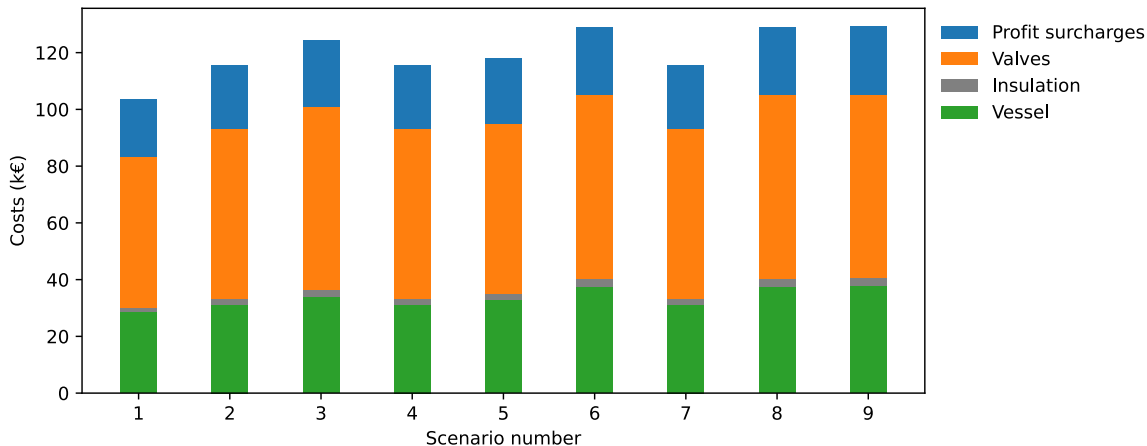


Fig. 14. Breakdown of storage non-discounted costs from the optimizations.

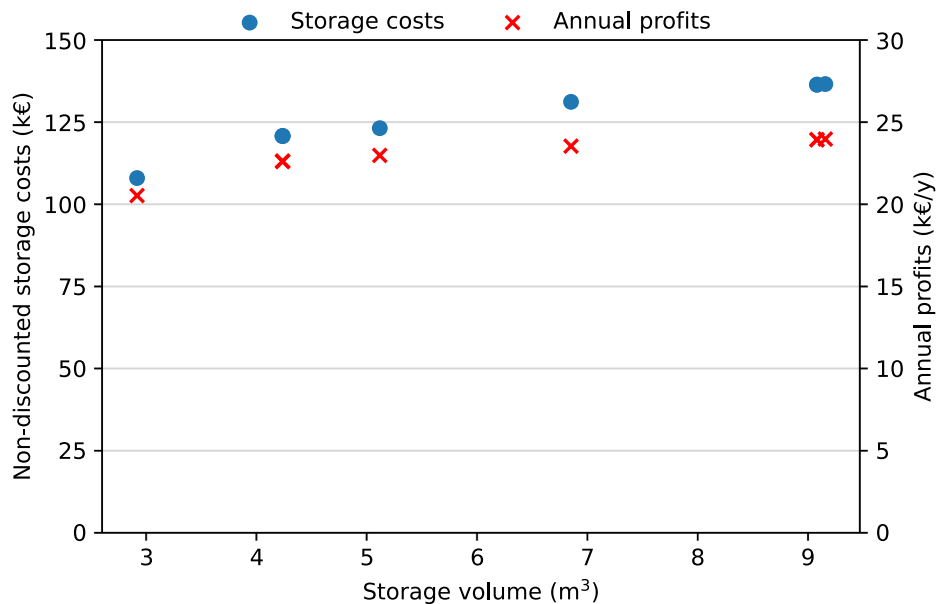


Fig. 15. Storage costs and profits for all nine scenarios.

For such relatively small pressure vessels, valve costs are the dominating factor and account for roughly half of the overall storage costs. Therefore, costs for the storage increase only slightly with storage volume and are characterized by decreasing specific costs. The storage costs and annual profits as a function of storage volume are shown in Fig. 15. The additional profits from increased storage size also flatten out with increasing volumes since the amount of recovered excess steam only increases slightly with increased storage volumes of the scenarios.

In the next section the simulation results using the design parameters from the techno-economic optimization in the simulation model are presented.

4.2. Simulated system performance

The charging and discharging times in the optimization procedure were based on perfect prediction, i.e., the whole period (one week) was known and optimized simultaneously. This is a common assumption in optimization analyses but can lead to overly optimistic results. The uncertainty of future events can play an important role for system control, especially when storages are involved. Therefore, the dynamic system was modeled without perfect prediction as explained in Section 3. All nine scenarios were parametrized and simulated separately to check the effect of the perfect prediction assumption. Simulation times for the analyzed week ranged from 10 to 40 min on an Intel® Core™ i7-8665U CPU with 1.90 GHz and 16 GB of RAM.

The simulated annual profits are around 4% lower than the optimization results for all scenarios (Fig. 16). In fact, the difference is about 0.9 k€/y for all nine scenarios (Table 3). The difference is caused by longer storage times (and the resulting increased losses), the limitation for discharging and the resulting decreased capacity, and the non-ideal control during system simulation. The difference in annual profits between optimization and simulation results are almost constant for all scenarios. The largest relative difference between optimization and simulation results are observed for scenario 1. It is expected that longer storage times and fewer charging and discharging cycles have a stronger negative effect on small storage vessels in comparison to the larger storage vessel in the other scenarios. The slightly reduced annual profits increase the payback time about 2 months in the simulated scenarios compared to the optimization results.

In fact, an important metric for storage use is the number of charging/discharging cycles. During the analyzed week, all scenarios show that the storage is charged around 400 times during both the simulations and the optimizations. However, the number of discharge activations vary significantly as shown in Fig. 17 (left).

It can be seen from Fig. 17 (left) that the number of discharge activations are around 400 for each scenario during the optimizations. The simulations on the other hand show a significantly lower number of discharge activations (around 200). Fig. 17 (right) also shows that the average discharging mass flow rate was higher during the simulations. A closer look at the results shows that this is due to the many small values of available excess steam in the measurement data. Because these are difficult to spot in Fig. 7, a load duration curve of all positive values is shown in Fig. 18.

Fig. 18 shows that around half of the measured values of excess steam mass flow rate are below 0.1 kg/s. The assumptions in the optimization procedure (purely energy-balance based) allows to charge the storage with these very small mass flow rates and to discharge immediately after charging. The more realistic control implementation in the simulation model only allows discharging when the pressure difference across the discharge valve exceeds 1 bar. Therefore, more steam has to be accumulated before discharging could be activated.

Transport and installation costs on-site were not included so far in the estimated payback times. A rough estimate would be in the order of 100 k€ according to plant operators. Discounted payback times for all scenarios including the estimated 100 k€ are listed in Table 4.

It can be seen that the payback periods are significantly higher compared to the values in Table 3 (2.8–5.8 years) due to the high installation costs. Also, the discount rate based on public funds is a significant factor for the payback periods in Table 4 and outweighs the difference between the optimized scenarios. In Norway, different governmental programs offer public funds that cover up to 50% for energy efficiency measures in industry when new technologies are introduced, so payback periods around seven years could be possible. However, a more detailed cost analysis is required to verify this.

5. Summary and conclusions

In this study, the impact of retrofitting a TES into an existing WHR system was analyzed. The aim of the TES was to increase the electricity production of the WHR system. A Ruths steam storage was chosen to mitigate the fluctuation of steam supply downstream of a drum boiler in a silicon production plant. In the Ruths steam storage, water is both the heat transport and heat storage medium, which is ideal when steam is stored over short periods. The Ruths steam storage was placed in parallel to existing bypasses to minimize interference of the retrofitted solution with the existing WHR system. Based on real data of a representative week from a silicon plant in Norway, a dynamic simulation model was calibrated. Afterwards, a techno-economic optimization was performed

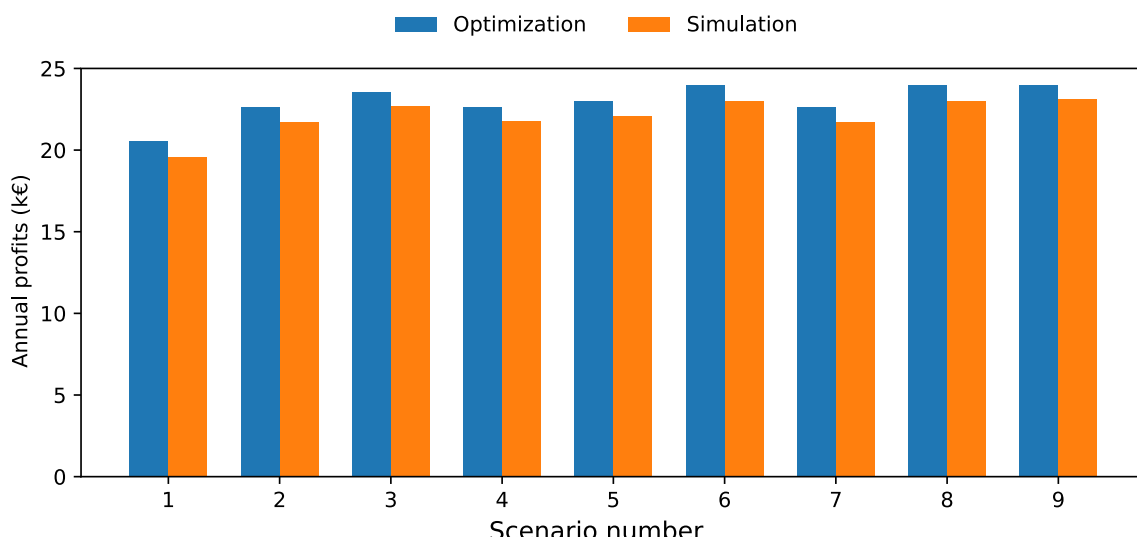
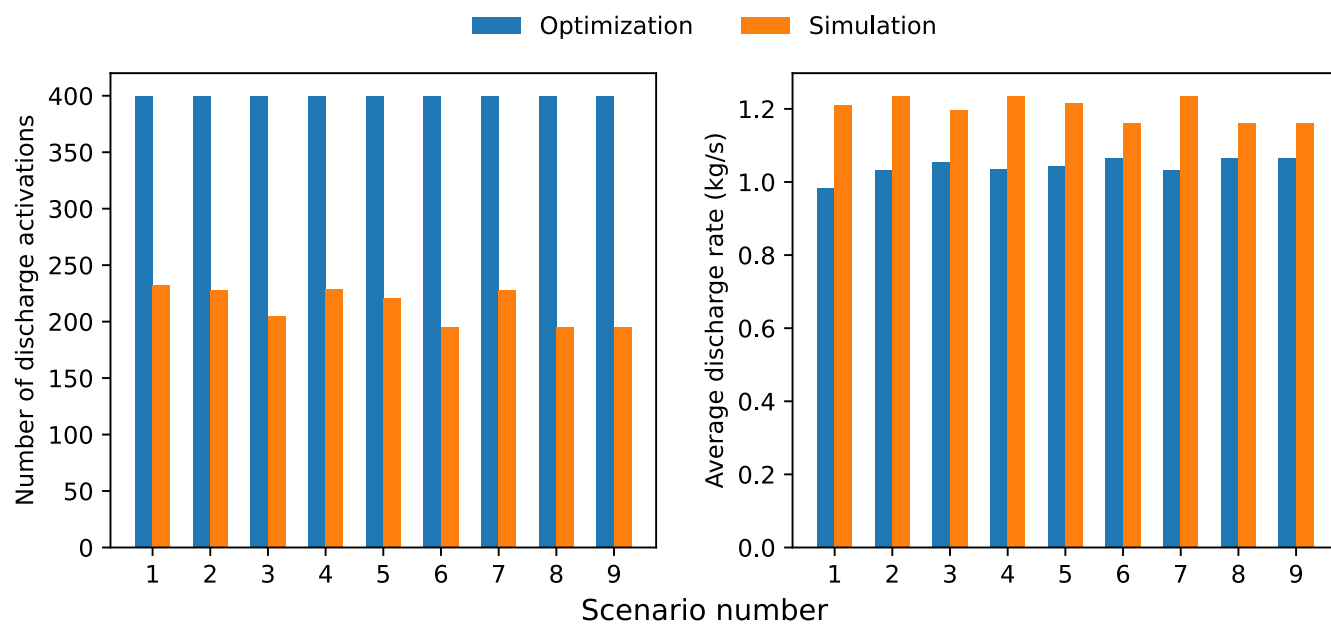
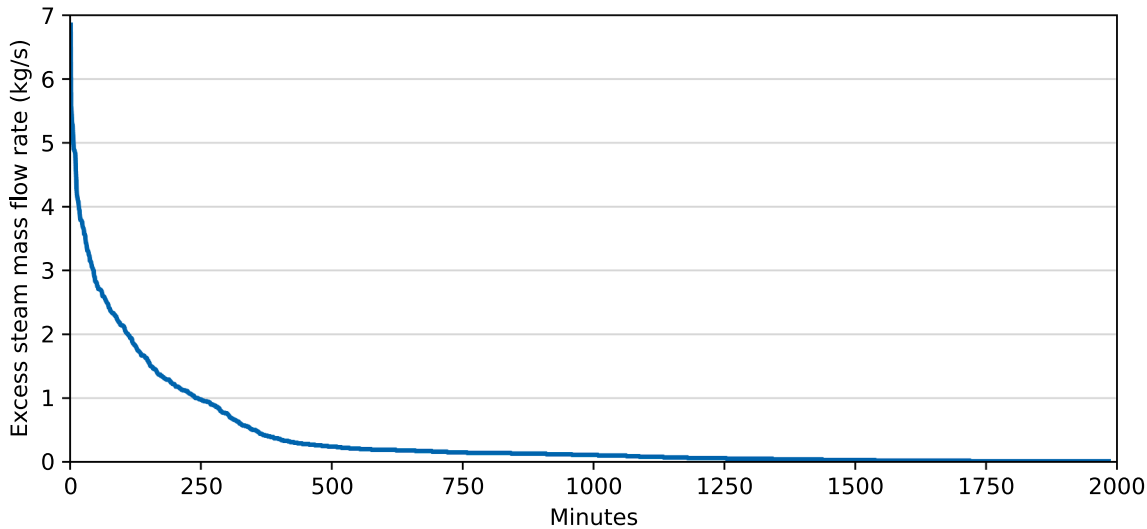


Fig. 16. Comparison of calculated annual profits from optimization and simulation.

Table 3

Economic results of TES in simulation.

Scenario Nr.		1	2	3	4	5	6	7	8	9
<i>Input parameters</i>										
Discount factor	%	0	0	0	20	20	20	50	50	50
Annualization period	y	5	10	15	5	10	15	5	10	15
<i>Economic Results</i>										
Annual profits	k€/y	19.6	21.7	22.7	21.8	22.1	23.0	21.7	23.0	23.1
Difference to optimization	k€/y	-0.9	-0.9	-0.9	-0.9	-0.9	-0.9	-0.9	-0.9	-0.9
Discounted payback time	y	5.5	5.6	5.8	4.4	4.5	4.7	2.8	3.0	3.0

**Fig. 17.** Storage operation during optimization and simulation for all nine scenarios (left: number of discharge activation, right: average discharging mass flow rate).**Fig. 18.** Load duration curve of the measured excess steam mass flow rate for the analyzed week.**Table 4**

Discounted payback periods including estimated installation costs.

Scenario Nr.		1	2	3	4	5	6	7	8	9
Discounted payback time	y	10.6	10.2	10.2	9.0	9.0	9.1	7.4	7.3	7.3

to optimize the design parameters of the Ruths steam storage based on the real plant data and data from the calibrated simulation model.

A Ruths steam storage model was added to the dynamic simulation model of the WHR system. A simple control strategy to charge and discharge the storage was implemented. The design parameters found in the techno-economic optimization were used in the dynamic simulation model to compare the performance of the retrofitted WHR system with the original WHR system. It was shown that the methodology to analyze and optimize the plant using a dynamic simulation model together with a techno-economic optimization increased the understanding of the system and helped to validate the optimization results. Moreover, similar performance could be reached with the simple control logic in the dynamic simulation model as in the techno-economic optimization.

It was shown that the installation of a storage volume of less than 10 m³ could reduce excess steam throttling significantly and increase the annual electricity production of the WHR system by 400–500 MWh, corresponding to annual profits of 20–23 k€. Non-discounted storage costs ranged from 108 to 140 k€, with transport and on-site installation not included. Including transport and on-site installation costs increased payback times significantly. Nevertheless, payback times of around seven years could be achieved with available public funds. Without public funds, payback times of about ten years are expected. Consequently, if just considering economic aspects, the small profit margin and long payback time might prevent the implementation of a Ruths steam storage in Elkem Thamshavn. These are similar challenges as reported by Dal Magro, Jimenez-Arreola [2].

However, the operation of the WHR system has been challenging due to the occurring temperature spikes. In addition, an expected change in raw material mix for the furnaces could lead to an even more fluctuating energy delivery to the drum-boiler in the near future. The implementation of a storage could therefore also be beneficial from an operational point of view, especially since a relatively simple control logic for storage operation was found to be sufficient in this study. Consequently, secondary objectives like increased component lifetime, which were not analyzed in this study, might make the presented TES system attractive for the operator of the considered silicon plant.

For future work, it is recommended analyzing longer time periods with a more detailed cost analysis also considering the benefits for the operations and component lifetime before making an investment decision. Moreover, besides cost-optimization also objectives such as maximizing exergetic use of excess heat and minimizing the carbon footprint of the WHR system could be considered. These different targets could also be considered within a multi-objective problem formulation.

Declaration of Competing Interest

The authors declare that they have no known competing financial interests or personal relationships that could have appeared to influence the work reported in this paper.

Acknowledgments

This work was funded by HighEFF - Centre for an Energy Efficient and Competitive Industry for the Future. The authors gratefully acknowledge the financial support from the Research Council of Norway and user partners of HighEFF, an 8-year Research Centre under the FME-scheme (Centre for Environment-friendly Energy Research, 257632/E20).

References

- [1] A. Schei, J.K. Tuset, H. Tveit, Production of High Silicon Alloys, Tapir Trondheim, 1998.
- [2] F. Dal Magro, M. Jimenez-Arreola, A. Romagnoli, Improving energy recovery efficiency by retrofitting a PCM-based technology to an ORC system operating under thermal power fluctuations, *Appl. Energy* 208 (2017) 972–985, <https://doi.org/10.1016/j.apenergy.2017.09.054>.
- [3] E. González-Roubaud, D. Pérez-Osorio, C. Prieto, Review of commercial thermal energy storage in concentrated solar power plants: Steam vs. molten salts, *Renew. Sust. Energy Rev.* 80 (2017) 133–148, <https://doi.org/10.1016/j.rser.2017.05.084>.
- [4] M. Trojan, D. Taler, P. Dzierwa, J. Taler, K. Kaczmarski, J. Wrona, The use of pressure hot water storage tanks to improve the energy flexibility of the steam power unit, *Energy* 173 (2019) 926–936, <https://doi.org/10.1016/j.energy.2019.02.059>.
- [5] M. Stark, F. Conti, A. Saidi, W. Zörner, R. Greenough, Steam storage systems for flexible biomass CHP plants – evaluation and initial model based calculation, *Biomass Bioenergy* 128 (2019) 105321, <https://doi.org/10.1016/j.biombioe.2019.105321>.
- [6] G. Nardin, A. Meneghetti, F. Dal Magro, N. Benedetti, PCM-based energy recovery from electric arc furnaces, *Appl. Energy* 136 (2014) 947–955, <https://doi.org/10.1016/j.apenergy.2014.07.052>.
- [7] A. Biglia, L. Comba, E. Fabrizio, P. Gay, D. Ricauda Aimonino, Steam batch thermal processes in unsteady state conditions: Modelling and application to a case study in the food industry, *Appl. Therm. Eng.* 118 (2017) 638–651, <https://doi.org/10.1016/j.applthermeng.2017.03.004>.
- [8] X. Yu, Z. Li, Y. Lu, R. Huang, A.P. Roskilly, Investigation of organic Rankine cycle integrated with double latent thermal energy storage for engine waste heat recovery, *Energy* 170 (2019) 1098–1112, <https://doi.org/10.1016/j.energy.2018.12.196>.
- [9] L. Miró, J. Gasia, L.F. Cabeza, Thermal energy storage (TES) for industrial waste heat (IWH) recovery: a review, *Appl. Energy* 179 (2016) 284–301, <https://doi.org/10.1016/j.apenergy.2016.06.147>.
- [10] T. Keplinger, M. Haider, T. Steinparzer, P. Trunner, A. Patrejko, M. Haselgrübler, Modeling, simulation, and validation with measurements of a heat recovery hot gas cooling line for electric arc furnaces, *Steel Res. Int.* 89 (6) (2018) 1800009, <https://doi.org/10.1002/srin.201800009>.
- [11] T. Steinparzer, M. Haider, A. Fleischanderl, A. Hampel, G. Enickl, F. Zauner, Heat exchangers and thermal energy storage concepts for the off-gas heat of steelmaking devices, *J. Phys.: Conf. Ser.* 395 (2012) 012158, <https://doi.org/10.1088/1742-6596/395/1/012158>.
- [12] W. Sun, Y. Hong, Y. Wang, Operation optimization of steam accumulators as thermal energy storage and buffer units, *Energies* 10 (1) (2016) 17, <https://doi.org/10.3390/en1001017>.
- [13] A. Gil, M. Medrano, I. Martorell, A. Lázaro, P. Dolado, B. Zalba, L.F. Cabeza, State of the art on high temperature thermal energy storage for power generation. Part 1—Concepts, materials and modelling, *Renew. Sust. Energy Rev.* 14 (1) (2010) 31–55, <https://doi.org/10.1016/j.rser.2009.07.035>.
- [14] M. Stark, M. Sonnleitner, et al., Approaches for Dispatchable Biomass Plants with Particular Focus on Steam Storage Devices, *Chemical Engineering & Technology* 40 (2) (2017) 227–237, <https://doi.org/10.1002/ceat.201600190>.
- [15] W.-D. Steinmann, M. Eck, Buffer storage for direct steam generation, *Solar Energy* 80 (10) (2006) 1277–1282, <https://doi.org/10.1016/j.solener.2005.05.013>.
- [16] F. Bai, C. Xu, Performance analysis of two-stage thermal energy storage system using concrete and steam accumulator, *Appl. Therm. Eng.* 31 (14) (2011) 2764–2771, <https://doi.org/10.1016/j.applthermeng.2011.04.049>.
- [17] E. Xu, Z. Wang, G. Wei, J. Zhuang, Dynamic simulation of thermal energy storage system of Badaling 1 MW solar power tower plant, *Renew. Energy* 39 (1) (2012) 455–462, <https://doi.org/10.1016/j.renene.2011.08.043>.
- [18] S.J. Liu, D. Faillé, M. Fouquet, B. El-Hefni, Y. Wang, J.B. Zhang, Z.F. Wang, G. F. Chen, R. Soler, Dynamic simulation of a 1MWe CSP tower plant with two-level thermal storage implemented with control system, *Energy Proc.* 69 (2015) 1335–1343, <https://doi.org/10.1016/j.egypro.2015.03.139>.
- [19] V. Samson Packiaraj Raphael, R. Velraj, P. Jalilah, Transient analysis of steam accumulator integrated with solar based MED-TVC system, *Desalination* 435 (2018) 3–22, <https://doi.org/10.1016/j.desal.2017.12.045>.
- [20] M. Richter, G. Oeljeklaus, K. Görner, Improving the load flexibility of coal-fired power plants by the integration of a thermal energy storage, *Appl. Energy* 236 (2019) 607–621, <https://doi.org/10.1016/j.apenergy.2018.11.099>.
- [21] B. Benalcazar, Sizing and optimizing the operation of thermal energy storage units in combined heat and power plants: an integrated modeling approach, *Energy Convers. Manage.* 242 (2021) 114255, <https://doi.org/10.1016/j.enconman.2021.114255>.
- [22] E. Pérez-Iribarren, I. González-Pino, Z. Azkorra-Larrinaga, I. Gómez-Ariarán, Optimal design and operation of thermal energy storage systems in micro-cogeneration plants, *Appl. Energy* 265 (2020) 114769, <https://doi.org/10.1016/j.apenergy.2020.114769>.
- [23] A. Pizzolato, F. Donato, V. Verda, M. Santarelli, A. Sciacovelli, CSP plants with thermocline thermal energy storage and integrated steam generator – techno-economic modeling and design optimization, *Energy* 139 (2017) 231–246, <https://doi.org/10.1016/j.energy.2017.07.160>.
- [24] R. Hofmann, S. Dusek, S. Gruber, G. Drexler-Schmid, Design optimization of a hybrid steam-PCM thermal energy storage for industrial applications, *Energies* 12 (5) (2019) 898, <https://doi.org/10.3390/en12050898>.
- [25] K. Lepiksaar, V. Masatin, E. Latosov, A. Siirde, A. Volkova, Improving CHP flexibility by integrating thermal energy storage and power-to-heat technologies into the energy system, *Smart Energy* 2 (2021) 100022, <https://doi.org/10.1016/j.segy.2021.100022>.
- [26] A. Beck, A. Sevault, G. Drexler-Schmid, M. Schöny, H. Kauko, Optimal selection of thermal energy storage technology for fossil-free steam production in the processing industry, *Applied Sciences* 11 (3) (2021) 1063, <https://doi.org/10.3390/app11031063>.

- [27] M. Takla, N.E. Kamfjord, H. Tveit, S. Kjelstrup, Energy and exergy analysis of the silicon production process, *Energy* 58 (2013) 138–146, <https://doi.org/10.1016/j.energy.2013.04.051>.
- [28] E. Ringdalen, M. Tangstad, *Softening and Melting of SiO₂, an Important Parameter for Reactions with Quartz in Si Production*, 10.1007/978-3-319-48769-4_4, Springer International Publishing, 2016, pp. 43–51.
- [29] M. Tangstad, Metal production in Norway. Metal production in Norway, Akademika Publishing, Trondheim, 2013.
- [30] K. Almås, H.K. Delbeck et al., Improved environmental and energy recovery performance with new furnace hood design at Elkem Thamshavn, in: *Silicon for the Chemical Industry VI*. Loen, Norway, 2002.
- [31] D. Rohde, T. Andresen et al., Energy recovery from furnace off-gas: Analysis of an integrated energy recovery system by means of dynamic simulation, in: Rankine 2020 Conference. Glasgow, 2020. <<https://doi.org/10.18462/iir.rankine.2020.1174>>.
- [32] TLK-Thermo GmbH. <<https://www.tlk-thermo.com/>>.
- [33] S. Dusek, R. Hofmann, A hybrid energy storage concept for future application in industrial processes, *Therm. Sci.* 22 (5) (2018) 2235–2242, <https://doi.org/10.2298/TSCI171230270D>.
- [34] S. Dusek, R. Hofmann, Modeling of a hybrid steam storage and validation with an industrial Ruths steam storage line, *Energies* 12 (6) (2019) 1014, <https://doi.org/10.3390/en12061014>.
- [35] DACE Cost and Value, DACE Price Booklet, edition 34: Cost information for estimation and comparison, 34 ed., Vakmedianet BouwCommunities B.V. 182, 2017.